25th Australasian Conference on Mechanics of Structures and Materials (ACMSM25)
Edited by C.M. Wang, J.C.M. Ho and S. Kitipornchai
Brisbane, Australia, December 4 – 7, 2018

PERFORMANCE OF BRIDGES WITH DAMAGED ELEMENTS IN EXTREME FLOOD EVENTS

W. Lokuge*, C. Fraser and W. Karunasena

School of Civil Engineering and Surveying, University of Southern Queensland, Springfield campus, QLD 4300, Australia

Emails: Weena.lokuge@usq.edu.au, u1032756@umail.usq.edu.au, karu.karunasena@usq.edu.au

*Corresponding author

Abstract. *Recent floods in Southeast Queensland, Australia have caused detrimental impacts on the social, environmental and economic aspects of the country. Bridges are considered as critical infrastructure because in a time of a disaster and during its recovery stage, bridges provide access for emergency services to flood affected communities. A community has the potential to be isolated if a bridge crossing a river or creek is damaged by flooding. Therefore it is important to understand the impact that flooding has on bridges so that they can be made less vulnerable to damage from these extreme events. In order to analyse the effects of flooding, a finite element model of a case study bridge was created using the software package Strand7. The flood loads determined by the Australian Standards were applied to a case study bridge (Tenthill Creek Bridge near Gatton in the Lockyer Valley, Queensland). Damage to the bridge was also simulated by adding weakened elements to the main structural elements of the bridge. In order to compare different load cases and damage scenarios performance indicators were used to assess the vulnerability. It was found that a damaged girder subjected to log impact loading produced the maximum stress in the bridge.*

Keywords: Floods; Infrastructure; Bridge failure; Resilience; Impact load

1 INTRODUCTION

In the recent past, there have been some notable floods in Queensland which includes the 2011 and the 2013 flood events. The 2011 flood was the most substantial flood to have occurred in recent history and also the most widespread. A heavy rainfall event combined with months of above average rainfall lead to the most catastrophic flood in Queensland in recent history. 2011 flood claimed 33 lives, caused $5 to $6 billion worth of damage to infrastructure and $350 million just for damages to bridges alone (Pritchard 2013). In January 2013 Tropical Cyclone Oswald, which developed in the Gulf of Carpentaria and crossed at the Cape York Peninsula as a Category 1 system, deteriorated to a tropical low pressure system and started moving south along the Queensland coast. Major flooding was seen in the Capricornia region of Queensland where record flood levels occurred. This flood claimed six lives and affected 54 council regions throughout the state. Critical infrastructures provide access across rivers, creeks and floodways, and they are quite essential to sustain normal activities (Oh, Deshmukh et al. 2010). They are important during the flood event as well as in the recovery stage to ensure the resilience of the community that they have served.

The reported work on the relationship between the infrastructure and the community can be divided into two groups. One group investigates about the effect of failure of infrastructure on the functioning of the industries (Rinaldi, Peerenboom et al. 2001, McDaniels, Chang et al. 2007) while others develop disaster mitigation strategies based on decision support tools (Oh, Deshmukh et al. 2010). Bridge infrastructure plays an important role during an extreme flood event by means of providing fast access for evacuation and during the rebuilding period ensuring access to the affected areas. Vulnerability assessment of these bridges are important because the resilience of the community during an extreme event relies on the proper maintenance of these critical infrastructures. The focus of this study is to conduct a structural analysis of deteriorated bridges under flood loadings. Different types of damage scenarios are used to imitate the possible modes of failure for different bridge elements.

In an extreme flood event there are many ways a bridge could fail. Damage can occur to the superstructure which includes damage to the girders, deck and surface (McPerson 2011, Murray and Kemp 2011); damage to the substructure which includes piers, abutments (Ezeajugh 2014), bearings and to the peripheral zone such as approaches (Murray and Kemp 2011). Setunge et al. (2014) have developed a set of failure criteria for different components of a bridge due to flooding. In the most recent extreme flood events in Queensland, quite a large number of bridges were damaged due to flood waters.

2 METHODOLOGY

The methodology for this research includes modelling a case study bridge located in the Lockyer Valley region in Queensland, Australia using finite element analysis software, Strand7 (Strand7 2010). The flood loads from AS 5100.2 (water, debris and impact forces) were applied to the bridge and in order to simulate localised failure or damage, an element or part of an element was removed from the model. The stresses and displacements were observed and were compared to the safe ranges for the specific material to determine if overall failure had occurred. The Strand7 output offers a range of result options in terms of different types of stresses and forces that can be analysed. The stresses considered in this research paper are the Von Misses Stresses as they represent the overall effects.

The main material used in the bridge model was reinforced concrete. If the compressive strength of concrete is exceeded then it will be crushed (CCAA, 2002). Australian standard for concrete structures, AS 3600 (Australia 2009), indicates that for any concrete member the deflection limit is span/250 while for members subjected to vehicular or pedestrian traffic, the limit is span/800.

3 CASE STUDY- TENTHILL CREEK BRIDGE

The selected bridge for the case study is located on the Gatton-Helidon Road and crosses Tenthill Creek in the Lockyer Valley region in Queensland, Australia. The bridge was constructed in 1976 and up until 1989, when the Gatton Bypass was opened; it was part of the Warrego Highway which carried traffic from Brisbane to Toowoomba. The Tenthill Creek Bridge is a simply supported reinforced concrete bridge with three 27.38 m spans and an overall length of 82.14 m and a width of 8.6 m. The height from the stream bed to the bridge is approximately 15.3 m. The dimensions for this bridge were obtained from the original plans from the Department of Main Roads Queensland. Using these dimensions, a simplified finite element model was created in Strand7. It is reported that the maximum flood for the bridge was approximately at the road surface level resulting in a velocity of 2.32 m/s (Setunge 2004).

3.1 Finite Element Model Development

Due to the size of the bridge, a larger mesh size had to be used in order to save on computing time. Each 27.38 m span was broken in to 15 segments. Across the width of the bridge there were 57 segments. Overall this gave a total of 12,714 brick elements. The model was completed in two parts. Firstly the deck and girder were assumed to be cast monolithically together in that it is one continuous unit. The piers and headstock were then added to the model. Link elements were used to attach nodes on the underside of the girder to nodes on the top of the headstocks. Master-slave link elements were used for this purpose where the nodes which they connect are forced to share the same displacements. The girders were assumed to be simply supported by the bridge abutments. Therefore these nodes were fixed in the horizontal and vertical directions, but rotation was allowed on the axis perpendicular the bridge girders. The girder node restraints are shown in Figure 1.

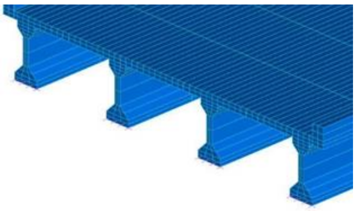

Figure 1 Girder nodal restraints at abutments

The footing of the piers was assumed to be fixed to simulate the piles that would normally be attached. A face support was applied around the footing to represent the surrounding soil. A value of 32000 kN/m^3 was used for the modulus of subgrade reaction, which represents a clayey medium dense sand (Strand7 2010). The modulus of subgrade reaction defines the relationship between the soil pressure and the deflection at the contact interface. The applied face support and footing nodal restraint are shown in Figure 2. The material used was reinforced concrete. According to the bridge technical drawings by Main Roads Queensland, the strength of concrete used for the case study bridge was 20 MPa. The modulus of elasticity, Poisson's Ratio and specific weight of concrete were taken as 25000 MPa, 0.2 and 24 kN/m^3 respectively.

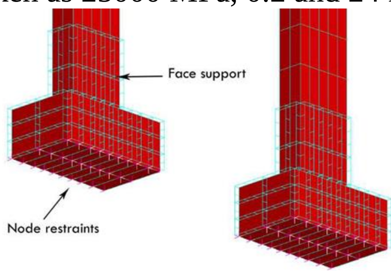

Figure 2 Pier node restraints and face support

3.2 Flood Data

Flood data was obtained from the Department of Natural Resources and Mines, Water Monitoring Portal. Streamflow data was available for the Tenthill Creek Stream gauge, which is located approximately 11 km upstream from the subject bridge. The maximum recorded flood at this stream gauge in 2013 had a peak discharge of 1359 m^3/s. This flood would have been associated with the ex-Tropical Cyclone Oswald event. The second highest flood in 2011, had a peak discharge of 1098 m^3/s. The probability of these flood events was estimated to be between 1 in a 100 year event to a 1 in a 500 year event (Rogencamp and Barton 2012). As this flood has a probability more than a 1 in 2000 year event, an ultimate load factor must be applied as per the standard and calculated to be 1.5. For a 20 year event, which was used for the serviceability limit states flood, Palmen-Weeks formula was used to determine the flow (Palmen, Weeks et al. 2011). A catchment area of 447 km^2 and a 72 hour, 50 year rainfall intensity of 3.54 mm/hr was used. From this the estimated Q_{20} flow was 601 m^3/s.

3.3 Applied Loads

Flood loads for the Tenthill Creek Bridge were determined for both the ultimate and serviceability limit states. Manning's Equation was used to determine the velocities of the floods (Equation 1).

$$V = \frac{1}{n} R^{2/3} S_f^{1/2} \quad (1)$$

Where *n* is the Manning's roughness coefficient, *R* is the hydraulic radius and S_f is the slope of the channel. The slope of the creek was estimated using the path feature in Google Earth, where an average channel slope was determined to be 0.2% or a grade of 1:500. The hydraulic radius was determined from the channel cross sectional area and the wetted perimeter for the required flood depth. The Manning's *n* value was estimated from the Modified Cowan Method (Brisbane City Council, 2003) as 0.069. The ultimate flood velocity was determined to be 2.3 m/s. This matches the stated maximum recorded flood velocity as mentioned earlier. The serviceability flood velocity was estimated as 1.9 m/s based on a discharge of 601 m^3/s. From the Manning's Equation, the flood depth was determined to be 4.5 m below the girder soffit.

3.3.1 Flood loads

The flood loads were calculated using AS 5100.2 and shown in Table 1. All flood loads indicated in the standard have been determined and detailed analysis was conducted to observe how they would affect the bridge for different states of damage.

Table 1 Calculated flood loads - Tenthill Creek Bridge

Load type	Ultimate	Serviceability
Drag force (F_{du})	907.86 kN	-
Lift force (+ve) (F_{Lu})	1801.05 kN	-
Lift force (-ve) (F_{Lu})	-6003.6 kN	-
Drag force (pier) (F_{du})	38.05 kN	8.71 kN
Lift force (pier) (F_{Lu})	53.44 kN	12.46 kN
Moment (M_{au})	2023.08 kN.m	-
Debris	1955.6 kN	-
Debris (pier)	-	368.22 kN
Log impact	158.7 kN	72.2 kN
Buoyancy	2938.68 kN	-

The location of the impact force on the girder was also analysed to determine if any other locations provided an adverse effect compared to being applied to the centre of the internal bridge span. These locations are at the centre of the inner and outer span, at the abutments and above the headstock.

3.3.2 Traffic Loads

The traffic load under the serviceability flood load was also analysed under different combinations to determine which has the most adverse effect. The S1600 and M1600 traffic loads were applied to both lanes of the bridge. The load combinations used were both lanes on outside span, one lane outside one lane inside, both lanes on inside span, and one lane on opposite outside spans.

3.4 Damage Scenario

The damage that will be applied to the case study bridge will include a weakened girder to represent damage due to debris load; a longitudinal crack applied to the web of the girder to simulate damage from an impact load; a pier crack and pier scour.

4 RESULTS AND DISCUSSION

The flood loads for ultimate and serviceability limit states, self-weight of the bridge, and traffic loads for serviceability were applied to the model in a number of combinations. The bridge was also analysed for a number of different states of damage including a weakened girder, girder cracking, pier cracking and pier scour.

4.1 Maximum Stress

The load cases for both serviceability and ultimate limit state flood events were compared and the maximum stress was obtained from the Strand7 model.

4.1.1 Undamaged state

The maximum Von Mises stress was obtained from the Strand 7 model for the undamaged state for each load case (51 combinations in total). For the traffic load combinations, the maximum stress value for each load category, i.e. hydrodynamic force, debris or impact, was obtained. From these results the maximum stress for the ultimate limit states occurred with the debris loading with a stress of 10.31 MPa. For serviceability limit states with water forces acting alone, the maximum stress of 6.29 MPa also occurred from the debris loading. Out of the traffic load combinations the stationary traffic load, combined with debris loading acting on the piers produced a maximum stress of 13.50 MPa. This was the highest stress out of all the load combinations. For the remaining analysis, only the S1600-1 traffic load will be used due to the data requirements and that it produces the highest stress. The S1600-1 load has the traffic load in both lanes on the outer span.

4.1.2 Weakened girder

A weakened girder was simulated by using a lower modulus of elasticity (100 MPa), but instead of being applied to a thin strip to simulate a crack, it was applied on a much wider section of the girder. The weakened girder acts to simulate a weakened section of the bridge, caused by a large impact load. The weakened girder scenario was applied to several locations on the bridge, including at the centre of the internal span, the centre of either outside spans, above the headstock supports and above the abutment support. Figure 3 shows an example of where the weakened girder has been applied above the headstock.

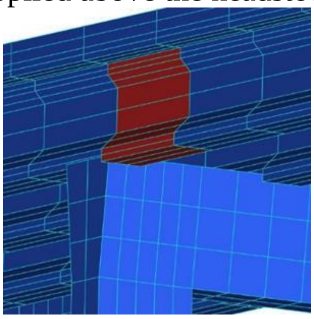

Figure 3 Weakened girder applied above headstock with 3 layers in depth

These locations were used as they would be where the maximum positive and negative moments occur in the girder and thus where the highest stresses will occur. The extent of the damage was also increased by increasing the depth of the weakened material properties. Three depths were used as the girders were divided into 3 elements in width. It can be observed that the maximum stresses are much higher for this damage state compared to the undamaged state.

4.1.3 Longitudinal cracking

For this damage state, horizontal cracks were added to the web of the girder to simulate a type of cracking observed in damaged bridges. This type of cracking would be caused by impact from large debris. Similar to the weakened girder in the previous section, small sections of the web were assigned a material property with a modulus of elasticity of 100 MPa. The crack spans approximately 7 m with a width of 50 mm and a depth of 100 mm. These were placed at various locations on the bridge. The cracks were also placed at the top, middle and bottom of the web to determine which case would cause the highest stress. The results were obtained for each load case and crack location on the bridge. The crack location which produced the highest stresses was on the outer span, at the top of the girder web

4.1.4 Pier scour

Scour around the pier was simulated in the model by removing the brick face support elements which were replicating the soil pushing against the face of the pier and footing. The pier scour was tested in two stages firstly with just the extent of scour to the top of the footing and then also with the whole footing exposed. From these results there is a negligible difference between just pier scour and scour of the pier and footing. This may be attributed to the support conditions used.

4.1.5 Pier cracking

Similar to the weakened girder, a section of the pier was assigned a material property with a lower modulus of elasticity to simulate a weakened or cracked pier. The weakened section was applied at the top, middle and bottom of the pier to see which location produced the most adverse effect. The weakened section was also applied in a number of layers. It was found that 4 layers of weakened material produced the highest stresses and for the remaining results only one and four layers were tested to save computing time. The process was repeated on the other pier. The weakened section applied to the centre of the right pier was found to give the highest stress. The traffic load in combination with the debris load produced the highest stress of 17.48 MPa.

4.1.6 Critical damage cases

From the Strand 7 results the damage scenario which produced the highest stress was the weakened girder applied above the headstock. The next critical damage state was the crack applied to the centre of the pier. Lastly, the longitudinal crack applied on the outer span adjacent to the headstock was also considered a critical case. Simulation of pier scour produced negligible effects to the maximum stresses. Further work on this pier scour analysis needs to be carried out in the future. In the present analysis, footing base nodes were assumed to be fixed. In future work, this condition needs to be relaxed by incorporating some sort of partial fixity or by partially allowing scour underneath the footing.

4.2 Cross Sectional Stresses

Further analysis was conducted on the results in the previous section. The critical load combinations and damage states were used for the analysis. The cutting plane feature of Strand 7 was used to analyse various cross sections along the bridge length. The areas of interest were those where the highest stresses were located and also where the damaged bridge sections were applied.

4.2.1 Undamaged bridge

The cross-section for the undamaged state under the ultimate debris load is shown in Figure 4 with von Mises stresses and σ_{xx} stresses. The σ_{xx} stresses shows the stress normal to the x-axis and in the direction of the x axis. In the model the flood loads are applied along the x-axis.

From Figure 4 a high area of stress occurs around base of the pier on the downstream side. This is from the debris load pushing the bridge clockwise about the base, creating stress concentrations in the corner of the pier and footing. In Figure 4 it can be seen that a tensile stress concentration occurs in the headstock. Again this is caused by the debris load pushing the bridge clockwise about its base. This type of stress has the potential the cause cracking in the headstock, although this type of damage has not been taken into account in this analysis.

4.2.2 Weakened girder

The weakened girder damage state produced the highest stresses out of all the other scenarios. The peak stress occurred with the ultimate impact load being applied directly to the section of weakened girder above the headstock. A cross-section at this location is shown in Figure 5(a).

(a) von Mises stresses (b) σ_{xx} stresses

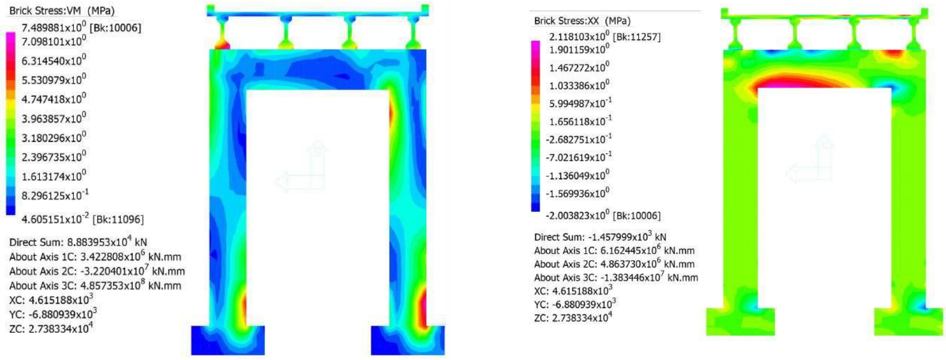

Figure 4 Undamaged bridge stresses under ultimate debris load

From this figure quite a high stress concentration occurs on the inside of the left most girder. This is where the damage has been applied. At this stage the damage has been applied to 2/3 of the overall thickness of the girder. Therefore the undamaged part of the girder is bearing the majority of the stress.

4.2.3 Longitudinal crack

The peak stress for this damage case occurred when the horizontal crack was located on the outer span adjacent to the headstock, with the crack being located at the top of the web. The loading case for this scenario was the traffic load in combination with the pier debris load. Below in Figure 5(b), a zoomed in cross-section of the deck and girder is shown with von Mises stresses used.

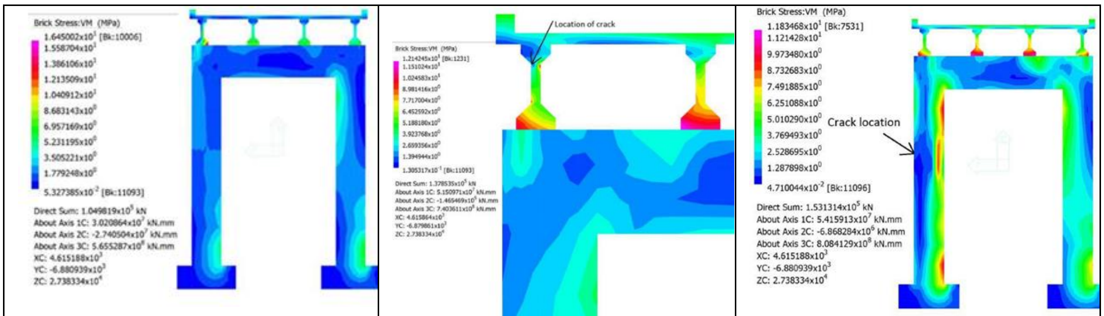

(a)Weakened girder- flood load (b)Longitudinal crack- traffic+debris (c)Pier crack- traffic+debris

Figure 5 Von Mises stresses

From the cross-section small areas of high stress are present in the top right corner of the web and bottom left corner of the web for the left girder. At these locations further cracking and damage is likely to occur if the load was to be increased.

4.2.4 Pier crack

The peak stress for the pier crack occurs when the crack is located at the centre of the pier under the traffic load combined with the pier debris load. Figure 5(c) shows the cross-section at which the crack is located. On the inside of the pier, opposite to where the crack is located, there is a relatively large strip of concentrated stress. This would be due to the cracked material on the outside of the pier not being able to effectively transfer the loads and forces. Thus this forces the stresses to be concentrated behind the crack, which may eventually lead to the crack worsening.

5 CONCLUSION

A thorough analysis has been conducted on how bridges behave under different flood loads and how they react when exposed to damage. A case study bridge located in the Lockyer Valley, Queensland, was used for the detailed analysis. The Tenthill Creek Bridge is a three span reinforced concrete bridge. A Strand 7 finite element model was created for this bridge and various flood loads such as hydrodynamic loads, debris loads, log impact loads were applied for both ultimate and serviceability limit states. A traffic loading was also applied in combination with serviceability loads. The case study bridge was also analysed with a number of damage scenarios including a weakened girder, longitudinal cracking of the girder, pier cracking and pier scour.

From the simulations it was determined that the impact loading caused the highest stresses to occur in the bridge. The damage this is likely to cause is cracking of the girder or of the pier, depending on where the impact load is occurring. The damage state which contributed to the highest stress was the weakened girder.

REFERENCES

Brisbane City Council (2003), Natural Channel Design Guidelines.

Cement and Concrete Association of Australia (2002), Guide to Concrete Construction. Sydney, Standards Australia.

Ezeajugh, L.E. (2014), Restoration of Scoured Out Bridge Approaches and Foundations - A QDTMR Perspective, Queensland Department of Transport and Main Roads.

McDaniels, T., S. Chang, K. Peterson, J. Mikawoz and D. Reed (2007), Empirical framework for characterizing infrastructure failure interdependencies, Journal of Infrastructure Systems 13(3), 175-184.

McPerson, R. (2011), Lockyer Valley Regional Council Infrastructure Damage and Inland Tsunami.

Murray, G. and A. Kemp (2011), Remediation of Bridges After the Queensland January 2011 Flood.

Oh, E., A. Deshmukh and M. Hastak (2010), Vulnerability Assessment of Critical Infrastructure, Associated Industries, and Communities during Extreme Events, Construction Research Congress 2010: Innovation for Reshaping Construction Practice, American Society of Civil Engineers.

Palmen, L., W. Weeks and G. Kuczera (2011), Regional flood frequency for Queensland using the quantile regression technique, Australian Journal of Water Resources 15(1), 47-57.

Pritchard, R. (2013), 2011 to 2012 Queensland floods and cyclone events: Lessons learnt for bridge transport infrastructure, Australian Journal of Structural Engineering 14(2), 167-176.

Rinaldi, S.E., J.P. Peerenboom and T.K. Kelly (2001), Identifying, understanding, and analyzing critical infrastructure interdependencies, IEEE Control System Magazine, 11-25.

Rogencamp, G. and J. Barton (2012), The Lockyer Creek Flood of January 2011: What Happened and How Should We Manage Hazard for Rare Floods, 52nd Annual Floodplain Management Authorities Conference, Floodplain Management Australia.

Setunge, S. (2004), Case Study: Comparison of current QDMR practices and applicability of FRP technology.

Setunge, S., W. Lokuge, H. Mohseni and W. Karunasena (2014), Vulnerability of road bridge infrastructure under extreme flood events, AFAC.

Standards Association of Australia (2009), Concrete Structures, AS 3600-2009.

Strand7 (2010), Using Strand7 - Introduction to the Strand7 Finite Element Analysis System. Sydney.